Surface Characterization of Modified Aluminas

I. The Lewis Acidity of Sm-Doped Al_2O_3

C. MORTERRA,*,1 G. MAGNACCA,* F. FILIPPI,† AND A. GIACHELLO†

*Dipartimento di Chimica Inorganica, Chimica Fisica e Chimica dei Materiali, Università di Torino, via P. Giuria 7, I-10125 Turin, Italy; and †Centro Ricerche Fiat, Strada Torino 50, I-10043 Orbassano Turin, Italy

The surface behavior of an alumina catalyst (support) containing ≈3 wt% Sm_2O_3 and fired at 773, 1273, and 1473 K has been investigated by IR spectroscopy and compared with the surface behavior of the corresponding undoped aluminas. It was observed that the addition of Sm, which at high temperatures stabilizes the transition (spinel) alumina phases, does not modify appreciably the spectral features of the surface hydrated layer (free surface OH groups), but modifies the Lewis surface acidity of the material. The ambient temperature adsorption of CO, pyridine, and CO_2 was investigated in some detail, and it was revealed that coordinatively unsaturated Sm centers progressively substitute, with increasing firing temperature, (all) the tetrahedrally coordinated Al centers in the surface layer. Spectral data indicate that the Lewis acidity of surface Sm^{3+} sites is intermediate between that of tetrahedrally and octahedrally coordinated surface Al sites. Samples activated under nonoxidizing conditions tend to present at the surface (relatively stable) reduced Sm centers. © 1992 Academic Press, Inc.

INTRODUCTION

The use of catalytic converters on gasoline-powered vehicles is becoming a worldwide reality. Converters consist of a ceramic/metallic support coated with a porous oxidic layer (washcoat), usually alumina, which contains catalytically active noble metal(s) and various additives. The most important properties of washcoats are high surface area and an open porosity so as to guarantee good contact with exhaust gases and high dispersion for the catalytic metal(s). For these reasons the washcoat layer is usually made of transition aluminas (e.g., γ- or δ-Al_2O_3).

At the beginning of converter life, the catalytic efficiency in the aftertreatment of exhaust gases is very high, but assuring the attainment of the limits over 80,000 miles of service is still a problem. There are several causes for the early aging of catalysts,

among which the most significant are the thermal deterioration of the washcoat layer and its chemical contamination (poisoning) due to oil trace components (e.g., P, Ca, Zn). In fact, high temperatures (≥1250 K) can result in the phase transformation of spinel transition aluminas into the stable trigonal form (α-Al_2O_3), characterized by low surface area and virtually no value as a catalyst and/or metal catalyst support. For this reason the washcoat of conventional three-way systems usually contains stabilizing additives (e.g., oxides of Ba or lanthanides), which tend to raise the temperature of the phase transition of alumina.

As for the contamination with some oil trace components, they can cause the well-known physical effect of pore blocking (1, 2), but they are also considered to interact with the alumina support on a (surface) chemical scale, yielding an earlier collapse of the support surface area and activity.

It was therefore decided to investigate, mainly by IR spectroscopy, the surface

1 To whom correspondence should be addressed.

properties of conventional catalytic aluminas modified by the addition of some oxides, either loaded deliberately as phase stabilizing agents or loaded to simulate the poisoning from oil components. The aim of this series of papers is to understand if there is a correlation (and to what extent) between the modifications of surface properties brought about by selected additives and the modifications that the additives produce in the texture (surface area and porosity) and structural (crystallographic) features of the starting alumina support.

This first contribution deals with the surface properties of a commercial catalytic alumina doped with small amounts of Sm oxide. The choice of Sm derives from the fact that several works dealing with the (bulk) properties of alumina doped with Ce or La oxides [e.g., Refs. (3–6)] have been reported, whereas no use has been made so far of the doping with Sm. On the other hand, due to its acid/base properties, Sm enters in the composition of several catalysts of high activity and selectivity [e.g., Refs. (7, 8)] and possesses at the same time general properties, like the possibility of two valence states, which are well representative of the whole family of lanthanides. It is recalled that mixtures of the latter are used most commonly as structural promoters and stabilizing agents against the thermal sintering of catalytic aluminas.

EXPERIMENTAL

Materials

Pure and Sm-doped alumina samples were prepared starting from two 10% water dispersions of pure commercial boehmite (Disperal Alumina, Condea Chemie). Under continuous stirring, a dosed amount of Sm nitrate solution was added to one of the dispersions to produce in the final calcined material an Sm_2O_3 concentration of 3% wt over Al_2O_3. The pH was adjusted in both dispersions to a final value of 3 by the addition of HNO_3. The suspensions were dried and heated at 353 K for 24 h, then the products were crushed in an agate mortar and given

TABLE 1

Surface Area and Crystal Phase Data of Pure and Sm-Doped Aluminas

Sample	A_{773}	A_{1273}	A_{1473}	ASM_{773}	ASM_{1273}	ASM_{1473}
BET surface area (m² g⁻¹)	186.5	120	4.5	156.5	140.5	17.5
Crystal phase	γ	δ (M)	α	γ	δ	ϑ (M)
		ϑ (m)				α (m)
						δ (vm)

Note. (M) Major comp.; (m) minor comp.; (vm) very minor comp.

a first oven treatment at 773 K for 3 h to convert γ-AlOOH into γ-Al_2O_3 (9).

Doped and undoped samples were fired in the air for 5 h at three temperatures (773, 1273, and 1473 K), rehydrated by exposure to the atmosphere for several days, and then prepared for IR measurements in the form of self-supporting pellets (15–25 mg cm⁻²). All thermal treatments were carried out at the chosen temperature in the IR cell, first *in vacuo* for 2 h (residual pressure ≤10⁻⁵ Torr; 1 Torr = 133.3 N m⁻²), and for the last 30 min in O_2 (≈100 Torr), unless otherwise stated.

Samples are designated in the text and figure captions by the symbols A (reference pure alumina samples) and ASM (Sm-doped samples), followed by a subscript numeral T_1 (K), representing the oven firing temperature of the material, and a second numeral T_2 (K), representing the temperature of vacuum thermal activation/oxidation undergone by the sample prior to adsorption and IR investigation.

BET surface areas determined with N_2 at 78 K with an automatic apparatus (Sorptomatic 1900, C. Erba) and the crystal phase data determined with an X-ray diffractometer (Philips PW 1050) are summarized in Table 1 and derive from a previous work concerning the preliminary characterization of numerous aluminas (10). In the starting γ-Al_2O_3 phase, the addition of Sm leads to an appreciable decrease of the BET surface area; this effect, for which we do not yet have a specific explanation (no systematic pore size distribution measurements have

been carried out) was observed to be produced by the addition of most lanthanide oxides and, in general, of several oxides of high specific weight that, in the separate oxide phase, possess a nonporous texture. Opposite to that, a stabilizing role played by Sm in respect to the surface area and crystal phase of the aluminas at high temperatures and, in particular, at the highest firing temperature adopted is quite evident.

IR Spectra

All spectra were run at resolution 2 cm^{-1} on a Bruker 113v FTIR spectrometer equipped with MCT detector. From all spectra of adsorbed CO and (end-on) CO_2, the contribution of the gaseous phase was computer-subtracted interactively. Segments of some unsmoothed spectra were band-resolved using an iterative Pascal program by Bruker (Simband), which fixes only the number of components to be resolved and the desired accuracy, whereas all other spectral parameters are allowed to float freely.

RESULTS AND DISCUSSION

Adsorption of CO

A. *Reference A samples.* The ambient temperature interaction of CO with transition aluminas has been investigated by IR spectroscopy some years ago (*11*) and has been reviewed more recently by Busca and Lorenzelli (*12*). It corresponds to the σ-dative coordination of a very limited number of CO molecules (the overall CO coverage at 300 K is far below 10% of a monolayer) onto highly coordinatively unsaturated (cus) surface cationic centers, possessing the tetrahedral coordination (Al_{cus}^{IV}) and acting as strong Lewis acidic sites. In fact, the IR spectrum of adsorbed CO presents bands in the 2200–2245 cm^{-1} interval, i.e., some 60–100 cm^{-1} above the frequency of gaseous CO, which implies a high degree of σ-charge release from the 5σ lone pair orbital of CO to the cus cationic centers.
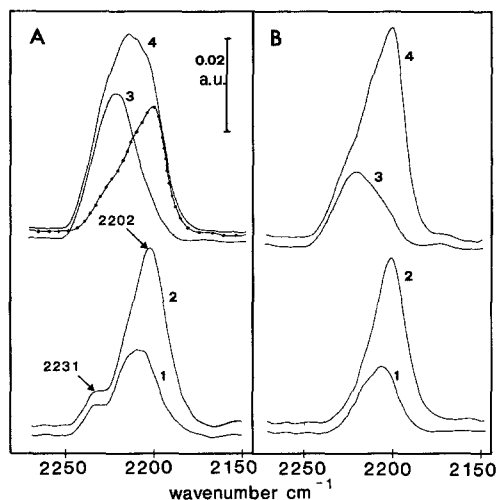
In the case of well-crystallized and pure-

Fig. 1. (A) Absorbance IR spectra of CO adsorbed on A_{773} samples. Curves 1 and 2: A_{773} 773 (P_{CO} = 5 and 50 Torr, respectively). Curves 3 and 4: A_{773} 1023 (P_{CO} = 5 and 50 Torr, respectively). Dotted curve (inserted for comparison): 50 Torr CO adsorbed onto A_{1273} 1023. (B) Absorbance IR spectra of CO adsorbed on A_{1273} samples. Curves 1 and 2; A_{1273} 773 (P_{CO} = 5 and 50 Torr, respectively). Curves 3 and 4: A_{1273} 1023 (P_{CO} = 5 and 50 Torr, respectively).

phase transition aluminas, the CO bands are two in number and relatively well resolved [for instance, the bands are at ≈2210 and ≈2240 cm^{-1}, respectively, on pure η-Al_2O_3 (*2*)], whereas in the case of structurally less defined aluminas the bands are probably more than two in number and appear much less resolved. This is the case, for instance, for the widely used Degussa alumina preparation termed Alon C (mainly δ-Al_2O_3) and is also the case for the microcrystalline alumina specimens (ex-boehmite) used in this work.

The adsorptive properties of the latter toward CO at 300 K, and at two CO coverages, are summarized in Fig. 1. Note in particular the following characteristics.

(i) In the starting γ-Al_2O_3 phase, isolated in a relatively low dehydration stage (curves 1 and 2 of Fig. 1A), two CO bands are resolved, centered at ≈2230 cm^{-1} (weak shoulder) and at ≈2200 cm^{-1} (broad and asymmetric), respectively, whereas in a

high dehydration stage (curves 3 and 4 of Fig. 1A) the whole 2250–2190 cm^{-1} spectral range is occupied by a broadish, asymmetric, and unresolved band. The latter indicates a highly heterogeneous distribution of coordinative and/or structural situations for the Al_{cus}^{IV} surface centres, active toward CO at ambient temperature.

(ii) In the δ,ϑ-Al_2O_3 phase (Fig. 1B), the CO band has become sharper and more asymmetric on the high $\bar{\nu}$ side, suggesting a modified distribution of the Al_{cus}^{IV} active centers. In particular, a selective elimination of the CO spectral components absorbing at the highest wavenumbers is noted ($\bar{\nu} \geq 2240$ cm^{-1}; for instance, compare curve 4 and the dotted trace in Fig. 1A), as well as a faster overall reversibility upon CO evacuation, indicating that in the so-called high-temperature transition aluminas (9) the Al^{IV} surface centers which, when dehydrated, possess the most uncoordinated configurations tend to become less and less abundant.

A consistent modification is noted in the spectral profile of the surface OH groups free from H-bonding, whose assignment has been long discussed, and is reported in the literature (13–15). Figure 2 (curves 1–3) shows that, after activation at the same temperature (773 K), A samples pretreated at increasing firing temperature exhibit a progressively decreasing relative intensity of one of the high-frequency OH components ($\nu_{OH} \approx 3775$ cm^{-1}). It is recalled here that the latter band has been ascribed by various authors to OH groups in the coordination sphere of Al^{IV} surface centers and was shown to be coupled with nearby (strong) acidic sites and to give rise, when eliminated upon dehydration, to the strongest Lewis acidic centers [see Ref. (15), and references therein].

(iii) For the alumina specimen oven fired at 1473 K, no CO spectra are reported, as no CO uptake is observed at any dehydration stage. This confirms that in the α-Al_2O_3 phase, where all bulk Al ions have the octahedral coordination (9) and, at the surface, only a few Al ions still exhibit a quasi-tetra-
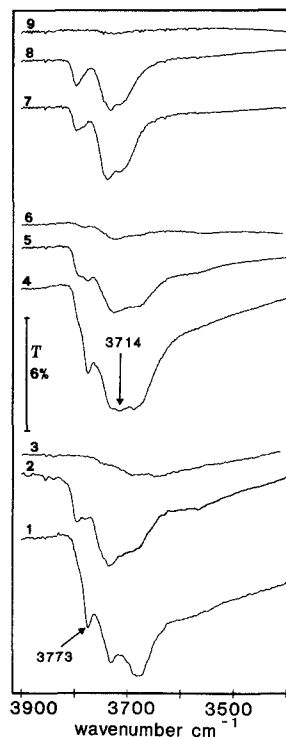

FIG. 2. Transmittance IR spectra of the free surface hydroxyl region of A_{T_i} and ASM_{T_i} samples. Curves 1–3: A_{773}, A_{1273}, and A_{1473} dehydrated at 773 K. Curves 4–6: ASM_{773}, ASM_{1273}, and ASM_{1473} dehydrated at 773 K. Curves 7–9: ASM_{773}, ASM_{1273}, and ASM_{1473} dehydrated at 1023 K.

hedral coordination (16), the surface Lewis acidity is not sufficient to σ-coordinate CO at ambient temperature.

B. ASM samples. The spectral patterns relative to the high-frequency region of ASM samples are shown in Fig. 2, curves 4–9; in addition to a shallow OH component at ≈ 3714 cm^{-1}, intermediate in frequency between two well-known OH components of pure aluminas (compare curves 1 and 4 of Fig. 2), no major differences are observed with respect to the corresponding patterns of the pure alumina systems (curves 1–3 of Fig. 2). In particular, an apparent decrease of the alumina OH band at ≈ 3680 cm^{-1} is probably due to the mentioned increased intensity of an OH component at ≈ 3714 cm^{-1}. These observations mean that no
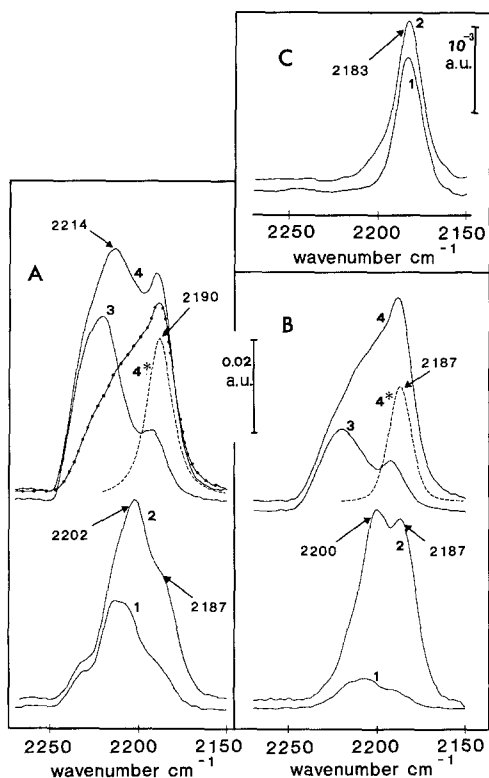
Fig. 3. (A) Absorbance IR spectra of CO adsorbed on ASM_{773} samples. Curves 1 and 2: ASM_{773} 773 (P_{CO} = 5 and 50 Torr, respectively). Curves 3 and 4: ASM_{773} 1023 (P_{CO} = 5 and 50 Torr, respectively). Broken curve 4*: a computer-resolved spectral component of curve 4. Dotted curve (inserted for comparison): 50 Torr CO adsorbed onto A_{1273} 1023. (B) Absorbance IR spectra of CO adsorbed on ASM_{1273} samples. Curves 1 and 2: ASM_{1273} 773 (P_{CO} = 5 and 50 Torr, respectively). Curves 3 and 4: ASM_{1273} 1023 (P_{CO} = 5 and 50 Torr, respectively). Broken curve 4*: a computer-resolved spectral component of curve 4. (C) Absorbance IR spectra of CO adsorbed on ASM_{1473} samples. Curves 1 and 2: 50 Torr CO on ASM_{1473} 773 and ASM_{1473} 1023, respectively.

bands due to OH groups to be specifically ascribed to surface Sm ions (i.e., located in the coordination sphere of surface Sm ions) can be singled out with certainty. Nevertheless, the spectra of adsorbed CO (as well as the spectra of other probe molecules) will indicate that the surface composition of aluminas has been appreciably modified by the presence of Sm.

Figure 3 summarizes some spectral fea-

tures of the ambient temperature interaction of CO with the Sm-doped alumina systems. The following characteristics can be noted.

(i) Already on the material fired at the lowest temperature and activated in mild conditions (curves 1 and 2 of Fig. 3A), the spectra of CO indicate the presence of a weak additional component centered at ≈ 2190 cm^{-1}, i.e., some 20 cm^{-1} lower than the lowest frequency CO component due to Al_{cus}^{IV} surface centers. The frequency of this CO band is still ≈ 45 cm^{-1} higher than that of gaseous CO and suggests that the adsorption involves the pure σ-dative coordination onto (non-d) cus surface cationic centers (Sm_{cus}^{3+}), acting as Lewis acidic centers of relatively high strength. This is a higher acidity, for instance, than that of Al_{cus}^{VI} centers, which cannot coordinate CO at ambient temperature and can only coordinate some CO at ≈ 78 K, yielding a weak band at a frequency as low as ≈ 2165 cm^{-1} (17).

On passing from ASM_{773} 773 to ASM_{773} 1023, the spectra of CO (curves 3 and 4 of Fig. 3A) indicate that, despite the lack of specific spectral evidence in the OH region, as reported above, an appreciable number of surface Sm ions were dehydrated, leading to an increased surface concentration of Sm_{cus}^{3+} sites. In fact, band resolution of the spectra of Fig. 3A indicates that, at P_{CO} = 50 Torr, the CO/Sm^{3+} component resolved at ≈ 2190 cm^{-1} (see curve 4 and the resolved component 4*) accounts for some 35% of the overall band of adsorbed CO, whereas it accounts for some 25% on the sample activated at lower temperature (curve 2).

(ii) On the material fired at 1273 K (curves 1–4 of Fig. 3B), a decline of the high-frequency CO components due to the strongest Al_{cus}^{IV} centers occurs, following the $\gamma \rightarrow \delta$ phase transition, much as occurs in the case of pure alumina. However, the CO spectrum is now dominated by the low $\bar{\nu}$ CO component ascribed to surface Sm_{cus}^{3+} centers; at P_{CO} = 50 Torr, the CO/Sm^{3+} component resolved at ≈ 2190 cm^{-1} (see curve 4 and the resolved component 4* in Fig. 3B) accounts for some 50% of the overall band

of adsorbed CO. Moreover, the effect of an increasing relative importance of the CO/Sm^{3+}_{cus} adspecies with activation temperature is even more evident on ASM_{1273} samples than it is on those of ASM_{773}.

The frequency of the CO/Sm^{3+}_{cus} σ-complexes is observed to shift to lower wavenumbers with increasing firing temperature.

(iii) On the ASM_{1473} system, the phase transition to α-Al_2O_3 is far from being complete in the bulk, as shown by the XRD spectra, so that some Al^{IV} sites, typical of the transition alumina phases, should still be present at the surface. Nevertheless Fig. 3C indicates that on ASM_{1473} virtually no Al^{IV}_{cus} activity toward CO is left, and the only CO band observed is that due to the σ-coordination onto Sm^{3+}_{cus} sites. The latter band is weak, due to the collapse of the surface area, and maintains a constant intensity for activation at $T \geq 773$ K. The band is now centered at ≈ 2183 cm^{-1}, i.e., some 7 cm^{-1} lower than the frequency at which it first appeared on the ASM_{773} (γ-Al_2O_3) system; this implies that, with firing, the structural and/or coordinative surroundings of the Sm^{3+}_{cus} adsorbing centers have changed somewhat, in the direction of a reduced overall charge withdrawing activity of the solid. In other words, this may mean that, with firing, a different (two-dimensional) phase has been produced at the surface of the Sm-Al_2O_3 system (e.g., a surface Sm aluminate) and that in this novel surface phase the degree of coordinative unsaturation achieved by Sm^{3+} centers is lower than when supported on the starting γ-alumina phase.

The OH spectra of Fig. 2 (compare curves 6 and 9) indicate that the sample $ASM_{1473}1023$ has become virtually fully dehydroxylated, but the thermal elimination of the last fraction of surface OH groups did not produce any appreciable increase of the strong Lewis acidity due to Sm^{3+}_{cus} centers. This means that during the last steps of dehydration, weaker acidic centers were probably produced, which may be revealed by

strong (hard) Lewis bases, but are not revealed by CO at 300 K.

C. Unoxidized ASM samples. When CO adsorption was carried out on ASM samples vacuum-activated at $T \geq 773$ K, but not oxidized, in addition to the CO bands at $\bar{\nu} \geq 2150$ cm^{-1} dealt with above, additional broad and asymmetric bands formed in the 2150–1800 cm^{-1} range (not shown). The detailed interpretation of these CO bands, the spectral position of which implies the presence of a back-donation contribution from the Sm adsorbing centers, is beyond the scope of this work and will be reported elsewhere. However, the formation of CO bands at $\bar{\nu} < 2143$ cm^{-1} is unexpected and suggests that on ASM preparations thermally activated in nonoxidizing conditions, relatively stable reduced Sm surface centers can form, which are not so commonly observed in a homogeneous phase (*18*). In some circumstances, this fact might have some effect on the catalytic behavior of Sm-containing alumina washcoat layers and of other Sm-containing catalytic systems.

In conclusion, the data relative to the CO adsorption at 300 K indicate that if the highest temperature experienced by the Sm-doped alumina catalysts is higher than ≈ 1300 K, the strong Lewis surface acidity of the system is mostly (and in the end exclusively) represented by cus Sm centers rather than by cus Al^{IV} centers. The cus Sm surface centers exhibit an oxidation state which depends reversibly on the oxidative/reductive properties of the catalytic medium.

Adsorption of Pyridine (py)

It is well known that, as an adsorbate, py is useful in distinguishing between Lewis and Brønsted acidity (*19*), but this use of py is not pertinent here, as no Brønsted acidity is exhibited by either pure or Sm-doped aluminas.

It is well known that py is a hard (strong) Lewis base and as such can be used in surface chemistry to differentiate surface Lewis acidic strength centers of different strength. In fact the surface acidic strength
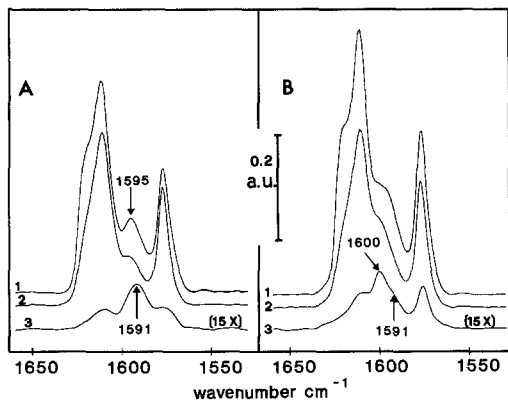
FIG. 4. (A) Absorbance IR spectra, in the pyridine 8a–8b "ring" stretching mode region, due to 8 Torr pyridine adsorbed onto A_{T_1} 1023 samples and evacuated at ambient temperature. Curve 1: A_{773} 1023. Curve 2: A_{1273} 1023. Curve 3: A_{1473} 1023 (the spectrum of curve 3 underwent a 15-fold Y-scale magnification). (B) Absorbance IR spectra, in the pyridine 8a–8b "ring" stretching mode region, due to 8 Torr pyridine adsorbed onto ASM_{T_1} 1023 samples and evacuated at ambient temperature. Curve 1: ASM_{773} 1023. Curve 2: ASM_{1273} 1023. Curve 3: ASM_{1473} 1023 (the spectrum of curve 3 underwent a 15-fold Y-scale magnification).

can range with continuity between that of the weakest charge-withdrawing sites (such as surface cus alkali metal ions or some surface OH groups capable of perturbing py by a plain H-bonding) and that of the strongest cus cationic sites (such as surface Zn^{2+}_{cus} cations in their regular tetrahedral coordination).

The most commonly used way to characterize the strength of Lewis-coordinated py is the observation of the IR spectral upward (blue) shift undergone by the 8a ring mode as a consequence of the N lone pair charge release to the adsorbing sites. The 8a ring mode, centered at ≈ 1580 cm^{-1} and almost unresolved from the partner 8b mode in liquid py, shifts to ≈ 1590 cm^{-1} in the case of a plain H-bonding (19) or of coordination to weak Lewis acidic sites [e.g., Al^{VI}_{cus} sites (16)], and can shift as much as to ≈ 1625 cm^{-1} in the case of coordination to very strong Lewis acidic centers [e.g., Zn_{cus} (20) or Al^{IV}_{cus} sites (15)].

Figure 4 reports the spectral region of the

8a–8b ring modes relative to the ambient temperature adsorption/evacuation of py on some A and ASM samples.

A. Reference A samples. Very little comment on the behavior of the reference A samples is needed, as the py/alumina(s) system has been extensively investigated by several authors. In Fig. 4A the following can be noted.

(i) The spectra of the γ phase (curve 1) and of the δ-ϑ phase (curve 2) are dominated by the 8a modes of the strong py complexes formed onto Al^{IV}_{cus} sites, absorbing at ≈ 1625 and ≈ 1615 cm^{-1}, respectively. The former species declines somewhat on passing from the γ to the ϑ-δ phase, confirming that the most uncoordinated (i.e., the strongest) Al^{IV}_{cus} centers become less abundant on the high-temperature transition phases, as already indicated in the previous section by the adsorption of CO.

(ii) On the γ and δ-ϑ phases, the 1605–1580 cm^{-1} spectral region contains a weak band (just a shoulder on A_{1273}), corresponding to few py species H-bonded to surface OH groups and/or coordinated to Al^{VI}_{cus} sites. Very few of the weak py/Al^{VI}_{cus} complexes are allowed to form in the presence of the abundant strong py/Al^{IV}_{cus} complexes, due to strong inductive effects from the latter. Moreover, most of the weak py/Al^{VI}_{cus} complexes are desorbed upon py evacuation at 300 K and are no longer observable under the conditions of Fig. 4A. The double nature of the weak py band observed on aluminas at ≈ 1590 cm^{-1} has been discussed elsewhere (21, 22).

(iii) After the phase transition to α-Al_2O_3, the overall spectral intensity of adsorbed py is very low, due to the collapse of surface area. Py uptake (curve 3 of Fig. 4A) reveals two adspecies: a minor amount of (quasi) tetrahedral sites (8a band at ≈ 1615 cm^{-1}), corresponding to cus $Al^{(IV)}$ centers which could not adsorb CO at ambient temperature, and an appreciable number of py/ Al^{VI}_{cus} complexes. The 8a mode of the latter species, broad and well resolved at ≈ 1590

cm^{-1}, is now easily observed in the virtual absence of py H-bonded to surface OH groups (in fact, A_{1473} 1023 is virtually fully dehydroxylated, as shown by curve 9 of Fig. 2) and in the presence of very few strong charge-releasing py/Al^{IV}_{cus} complexes.

B. ASM samples. The adsorption of py on ASM samples, reported in Fig. 4B, shows the following.

(i) The overall trend with firing temperature of the py/Al^{IV}_{cus} complexes parallels that exhibited by the pure alumina samples. This confirms the indications already given by the adsorption of CO, dealt with in the previous section.

(ii) On ASM samples fired at $T \leq 1300$ K, the 8a py band at $\bar{\nu} \leq 1600$ cm^{-1} (≈ 1595 cm^{-1}) exhibits a spectral position somewhat higher than on pure alumina, a broader and complex profile, and a relative intensity definitely higher with respect to the main absorption due to the py/Al^{IV}_{cus} complexes (especially in the case of ASM$_{1273}$; compare curves 2 in Figs. 4A and 4B). This suggests that one more component, of frequency higher than that in the case of alumina A samples, is probably contained in the 1605–1590 cm^{-1} band envelope.

The latter observation becomes quite clear on the fully dehydrated ASM$_{1473}$ 1023 sample (see curve 3 of Fig. 4B): in the 1605–1580 cm^{-1} range there is a sharp band centered at ≈ 1600 cm^{-1} (i.e., some 10 cm^{-1} higher than the broad band observed on A_{1473}) and a weak shoulder at ≈ 1590 cm^{-1}. The latter component can be ascribed to few py/Al^{VI}_{cus} complexes resisting evacuation (no H-bonded py can form in this case, as virtually no OH groups are left), whereas the main band at ≈ 1600 cm^{-1} is assigned to py Lewis coordinated to surface Sm^{3+}_{cus} centers.

Pyridine adsorption therefore confirms that:

(i) by increasing the firing temperature of the Sm-doped alumina catalyst, the Lewis acidity of the surface layer is represented more and more by cus Sm ions rather than by cus Al ions;

(ii) the Lewis acidity of Sm^{3+}_{cus} centers is

intermediate between that of Al^{IV}_{cus} and Al^{VI}_{cus} centers.

Adsorption of CO₂:
  End-on CO₂ Complexes

The picture of the surface Lewis acidity of Sm-doped aluminas given in the previous sections by the adsorption of CO and py is confirmed in this section by the adsorption of CO_2.

The adsorption of CO_2 at 300 K is known to occur on most oxidic systems through the formation of carbonate-like species (which reveal basic sites and acid–base pairs) and of linearly held end-on complexes (which reveal Lewis acidic surface sites). For this reason we think that the use of CO_2 adsorption/desorption as a specific tool for estimating quantitatively the plain surface basicity of solids [as recently performed, for instance, on some modified aluminas by Berteau *et al.* (*23*)] must be adopted with some caution.

The sensitivity of CO_2 adsorbed in the end-on linear form toward weak surface-acidic sites, and its suitability to differentiate strong and weak surface acidic centers, has recently been reported (*24*). One of the peculiar features of this weak adsorption mode (quite pertinent to the present discussion and shown for samples A in curves 1–3 of Fig. 5A) can be stated as follows. If at the surface of a nonconducting solid (i.e., a system with a limited capacity of receiving extra charge) more than one σ-coordinated end-on CO_2 species of different strength can form, and the activation conditions become such as to allow the formation of the stronger CO_2 end-on species, the amount of the weaker end-on complexes declines since they become inhibited by the presence of the stronger charge-releasing species. This effect (a surface inductive effect), which is valid in general (e.g., see the case of the py/Al^{VI}_{cus}–py/Al^{IV}_{cus} surface complexes, discussed above), is particularly evident in the case of end-on CO_2 complexes, due to the weakness of the relevant acid–base interaction.
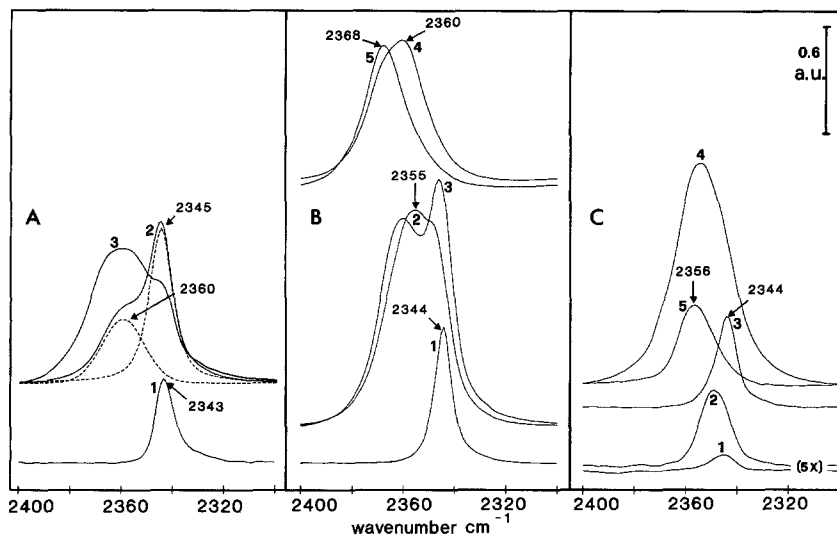
FIG. 5. (A) Absorbance IR spectra of CO_2 (15 Torr) end-on coordinated onto some A_{773} T_2 samples. Curve 1: A_{773} 423. Curve 2: A_{773} 773; broken curves: band-resolved components of curve 2. Curve 3: A_{773} 1023. (B) Absorbance IR spectra of CO_2 end-on coordinated onto some ASM_{773} T_2 samples and some reference A_{773} T_2 samples. Curve 1: 15 Torr CO_2 on ASM_{773} 423. Curve 2: 5 Torr CO_2 on ASM_{773} 773. Curve 3: 5 Torr CO_2 on the corresponding reference A_{773} 773 sample. Curve 4: 5×10^{-2} Torr CO_2 on ASM_{773} 1023. Curve 5: 5×10^{-2} Torr CO_2 on the corresponding reference A_{773} 1023 sample. (C) Absorbance IR spectra of CO_2 end-on coordinated onto some ASM_{1473} T_2 samples and some reference A_{1473} T_2 samples. Curves 1 and 2: 15 Torr CO_2 on A_{1473} 373 and A_{1473} 1023, respectively (spectra 1 and 2 underwent a 5-fold Y scale magnification). Curves 3 and 4: 15 Torr CO_2 on ASM_{1473} 373 and ASM_{1473} 1023, respectively. Curve 5: same as curve 4, after the evacuation of CO_2 to 5×10^{-2} Torr.

A. Reference A samples. Figure 5A is relative to the end-on adsorption of CO_2 onto some *A* reference samples, and shows that:

(i) after a vacuum activation at low temperatures (300–450 K, curve 1; at these temperatures only undissociated coordinated water desorbs from the alumina surface) very weak end-on CO_2 complexes, absorbing at $\approx$2343 cm^{-1}, start forming at Al_{cus}^{VI} sites;

(ii) after activation at intermediate temperatures (450–780 K; see curve 2 and the corresponding band-resolved broken curves), when more Al_{cus}^{VI} centers form and Al_{cus}^{IV} sites start forming upon dehydroxylation, other stronger end-on CO_2 complexes form, absorbing at $\bar{\nu} > 2350$ cm^{-1}, but the band relative to the CO_2/Al_{cus}^{VI} complexes, now centered at $\approx$2345 cm^{-1}, is still predominant;

(iii) after activation at $T \geq 850$ K (curve 3),

when the last stages of surface dehydration produce an appreciable number and a wider variety of Al_{cus}^{IV} centers (as previously shown by CO adsorption), the bands relative to the strongest CO_2 end-on complexes increase dramatically, and the intensity of the band at $\approx$2345 cm^{-1} due to the CO_2/Al_{cus}^{VI} complexes declines, being inhibited by the inductive effects from the stronger CO_2/Al_{cus}^{IV} complexes.

B. ASM samples. Curve 1 of Fig. 5B shows, for one of the Sm-doped systems, that the earliest stages of dehydration already liberate some Al_{cus}^{VI} centers, much as they do on pure aluminas, yielding CO_2 end-on complexes absorbing at $\approx$2345 cm^{-1}. This behavior is the same for all ASM_{T_i} systems (e.g., see curve 3 of Fig. 5C), but for the intensity of the bands, due to the changes of surface area. Curves 2–5 of Fig. 5B report a direct comparison of *A* and ASM

samples treated under the same conditions and CO_2 pressures. It can be noted that, depending on the temperature of activation and on the CO_2 pressure, when it is possible to observe CO_2 end-on complexes adsorbed onto both Al_{cus}^{VI} and Al_{cus}^{IV} centers (curves 2 and 3), on ASM samples there is an additional band at an intermediate frequency (≈ 2355 cm^{-1}), whereas under low CO_2 pressures (curves 4 and 5), when only the stronger end-on complexes can be observed, the band of CO_2/Al_{cus}^{IV} (≈ 2368 cm^{-1}) exhibits on ASM samples a major side component at lower frequency (≈ 2360 cm^{-1}), due to CO_2/Sm_{cus}^{3+} species.

These data show, even more clearly than in the case of CO and py uptake, that the formation of Sm_{cus}^{3+} sites at the surface of aluminas corresponds to the creation of Lewis acidic centers of intermediate strength between Al_{cus}^{IV} and Al_{cus}^{VI} sites.

Finally, Fig. 5C shows the following.

(i) On α-Al_2O_3, almost no activity toward CO_2 is exhibited in the early stages of dehydration (curve 1), whereas on the material fully dehydrated at high temperatures a weak, broad, and asymmetric band of CO_2/Al_{cus}^{VI} complexes forms at ≈ 2348 cm^{-1} (curve 2).

(ii) In the early stages of dehydration of ASM_{1473}, regular CO_2/Al_{cus}^{VI} complexes form, absorbing at ≈ 2344 cm^{-1} (curve 3; note that the use of CO_2 adsorption, yielding the end-on coordination, is once more vital in determining the presence of weak Lewis acidic centers), whereas on the material activated at high temperatures the spectrum of CO_2 end-on complexes is dominated by the band at ≈ 2356 cm^{-1}, ascribed to the adsorption onto Sm_{cus}^{3+} sites (see curves 4 and 5). In curve 4, the partner components on the higher and lower $\bar{\nu}$ side of the ≈ 2356 cm^{-1} band, due to CO_2/Al_{cus}^{IV} and CO_2/Al_{cus}^{VI} complexes, respectively, are virtually missing: the scarcity of the latter is mainly due to the (inductive) inhibition by the overwhelming amount of the stronger CO_2/Sm_{cus}^{3+} complexes (in fact curve 3 showed

that Al_{cus}^{VI} centers *do* form at the surface of ASM_{1473}), whereas the virtual absence of CO_2/Al_{cus}^{IV} complexes is due to the scarcity of the relevant sites at the surface of ASM samples fired at high temperatures, as already suggested by the adsorption of CO and Py.

CONCLUSIONS

The IR background spectrum of Sm-doped aluminas is insufficient per se in revealing the surface modifications brought about in the surface layer of transition aluminas by the addition of the foreign element. In fact only minor changes are seen in the surface OH composition, and no new background bands ascribable to different surface phases appear in any region of the mid-IR range. XRD data also exclude that different phases are formed in the bulk of the solid fired at $T \leq 1473$ K.

IR experiments on adsorption carried out with three selected probe molecules, each of which reveals some particular aspects of the surface-modified material, turn out to be quite useful in showing that the added Sm atoms tend to collect at the surface of the solid and, in doing so, modify the acid/base features of the uppermost layer of particles.

The presence of Sm oxide stabilizes, in the bulk of the solid, the transition (spinel) alumina phases, so that also on materials fired at temperatures as high as ≈ 1500 K the surface area is still of the order of some 15 m^2 g^{-1}, and the catalytically inactive corundum phase is still virtually absent. In this respect, the addition of Sm oxide to the alumina washcoat layer seems to be quite useful.

Nevertheless, the surface layer of Sm-doped aluminas does not behave any longer as the surface layer of transition aluminas, and this is more and more so the higher the temperatures of preliminary firing. In fact, with progressively higher firing temperature, the surface composition changes progressively and tends to a final situation in which probably a two-dimensional new phase (Sm aluminate) has been produced, although no separate phases of this type

could be observed. In this surface phase, (almost) no Al ions with a tetrahedral coordination are exposed anymore (and the latter are known to be the centers catalytically active at the surface of transition aluminas); the surface Lewis acidity is definitely lower, as it is now mainly represented by Al_{cus}^{VI} and Sm_{cus} ions. The latter species are characterized by a medium Lewis acidic strength and exhibit the regular $3+$ oxidation state of lanthanides when activated in an oxidizing environment, but a thermal activation at relatively low temperatures under nonoxidizing conditions (e.g., *in vacuo*) seems to be sufficient to stabilize reduced valence states of the Sm atoms. This fact, to be further investigated, may have some interesting implications for catalysis.

REFERENCES

1. Williamson, W. B., Perry, J., Gandhi, H. S., and Bomback, J. L., *Appl. Catal.* **15**, 277 (1985).
2. Joy, G. C., Molinaro, F. S., and Homeier, E. H., Soc. Automot. Eng., Technical report No. 852099, 1985.
3. Ozawa, M., Kimura, M., and Isogai, A., *J. Mater. Sci. Lett.* **9**, 709 (1990).
4. Kato, A., Yamashita, H., Kawagoshi, H., and Matsuda, S., *J. Am. Ceram. Soc.* **70**, C157–159 (1987).
5. Scaper, H., Doesburg, E. B. M., and van Reijen, L. L., *Appl. Catal.*, **7**, 211 (1983).
6. Beguin, B., Garbowski, E., and Primet, M., *Appl. Catal.* **75**, 119 (1991).
7. Otsuka, K., Jinno, K., and Morikawa, A., *J. Catal.* **100**, 353 (1986).
8. Choudhary, V. R., and Rane, V. H., *J. Catal.* **130**, 411 (1991).
9. Lippens, B. C., and Steggerda, J. J., *in* "Physical and Chemical Aspects of Adsorbents and Catalysts" (B. G. Linsen, M. H. Fortuin, C. Okkersee, and J. J. Steggerda, Eds.), p. 171. Academic Press, London, 1970.
10. Giachello, A., and De Maestri, P. P., CRF Technical Int. Report, No. 1083, 1990.
11. Della Gatta, G., Fubini, B., Ghiotti, G., and Morterra, C., *J. Catal.* **43**, 90 (1976).
12. Busca, G., and Lorenzelli, V., *Mater. Chem.* **7**, 89 (1982).
13. Peri, J. B., *J. Phys. Chem.* **69**, 220 (1965).
14. Knözinger, H., and Ratnasamy, P., *Catal. Rev. Sci. Eng.* **17**, 31 (1978).
15. Zecchina, A., Coluccia, S., and Morterra, C., *Appl. Spectrosc. Rev.* **21**, 259 (1985).
16. Morterra, C., Coluccia, S., Chiorino, A., and Boccuzzi, F., *J. Catal.* **54**, 348 (1978).
17. Zecchina, A., Escalona Platero, E., and Otero Areán, C., *J. Catal.* **107**, 244 (1987).
18. (a) Cotton, F. A., and Wilkinson, G., "Advanced Inorganic Chemistry," p. 986. Wiley, New York, 1980; (b) Greenwood, N. N., and Earnshaw, A., "Chemistry of the Elements," p. 1436, Pergamon, Oxford, 1984.
19. Parry, E. P., *J. Catal.* **2**, 371 (1963).
20. Morterra, C., and Cerrato, G., *Catal. Lett.* **10**, 357 (1991).
21. Morterra, C., Chiorino, A., Ghiotti, G., and Garrone, E., *J. Chem. Soc. Faraday Trans. 1* **75**, 271 (1979).
22. Morterra, C., and Cerrato, G., *Langmuir* **6**, 1810 (1990).
23. Berteau, P., Kellens, M.-A., and Delmon, B., *J. Chem. Soc. Faraday Trans.* **87**, 1425 (1991).
24. Morterra, C., Cerrato, G., and Emanuel, C., *Mater. Chem. Phys.* **29**, 447 (1991).